Air Stirring System for Adsorption of Hexavalent Chromium onto Chitosan

Mamdouh M.Nassar[(1)], Abd EL Hakim Daifullah[(2)], Joseph Y. Farah [(3)*] and H.Kelany[(1)]

Abstract - The adsorption of hexavalent chromium from aqueous solutions onto chitosan was investigated. The chitosan was characterized by Fourier transform infrared spectroscopy (FT-IR) and Scanning Electron Microscopy (SEM). The physical properties of chitosan were also investigated.
 The effect of chitosan mass, initial chromium concentrations and air flow rate on the removal of chromium in batch reactor using air stirring technique have been studied The experimental kinetic data were tested using Pseudo-first order, Pseudo-second order, Elovich and Modified Freundlich models. Three error functions were used to identify the best fit model with the experimental data. The error analysis showed that, compared with other models, the , Pseudo-second order model resulted in the lowest values for the error function and thus fitted the data better than the other models.
Keywords - Bubble column adsorber ; Hexavalent chromium ; Chitosan ; Kinetic modelling; Error analysis.

----

1. INTRODUCTION

THE industrial discharge of the heavy toxic metal ions into water recourses is a serious pollution problem affecting water quality. Among the heavy metal ions, chromium holds a distinct position due to its high toxic nature to biological systems. Chromium exists in the +III and +VI oxidation states in aqueous medium but Cr(VI) is 500 times more toxic than Cr(III)[1]. The toxicity of Cr(VI) is associated with lung cancer as well as kidney, liver and gastric damage [2,3].

Conventional methods applied for Cr (VI) removal are mainly chemical precipitation, oxidation/reduction, filtration, ion exchange, membrane separation and adsorption [4]. At present, one of the most promising treatment approaches for wastewater polluted by Cr (VI) is based on adsorption of Cr (VI) onto different adsorbents [5], as this method offers advantages including low cost, flexibility and simplicity of design, ease of operation, insensitivity to toxic pollutants and avoiding the formation of secondary pollutants [6].

Gas stirring is widely employed in many industrial applications as in reactors or gas-liquid contactors. The bubble columns have the advantages of being geometrically simple, easily manufactured, free of moving parts, superior for gas-liquid interfacial mass and heat transfer, easily operated and cost effective [7-9].

 Few authors use gas stirring in the adsorption column to remove pollutants from waste water. In the present study, we use air stirring system to remove hexavalent chromium from water [10-12].

_____

1. *Chemical Engineering Department, Faculty of Engineering , EL-Minia University ,EL-Minia, Egypt.*
2. *Hot Laboratory and Waste Mangement Centre ,Atomic Energy Authority,Egypt.*
3. *Chemical Engineering and Pilot Plant Department National Research Centre*
* *Co-Author E-mail: josephyfarah@hotmail.com*

2. MATERIALS AND METHODS

2.1 MATERIALS

All the chemicals used in our experiments were of analytical grade, chitosan [$(C_6H_{11}NO_4)_n$] which has molecular weight 100,000 – 300,000 and supplied from Acros Organics – New York, USA. Potassium dichromate ($K_2Cr_2O_7$, 99.5% Assay – M.W.294.18) was obtained from LOBA CHEMIE PVT. LTD. INDIA.

Stock solution of Cr(VI) (130 mg/dm³) was prepared by dissolving $K_2Cr_2O_7$ salt in double distilled water and the concentration of Cr(VI) in the stock solution was measured. Experimental solutions at the desired concentrations were then obtained by successive dilutions. Before adding the sorbents, the pH of each test solution was adjusted to the required value with 0.1 M HNO_3 and 0.1 M NaOH. The concentration of free chromium ions in the stock solutions and unadsorbed Cr(VI) in the reaction medium was determined spectrophotometrically at 540 nm in a spectrophotometer using 1,5 diphenylcarbazide (OXFORD Laboratory Reagent – $C_{13}H_{14}ON_4$ – M.W. 242.28) as the complexing agent [13,14] .

2.2 METHOD OF MATERIAL CHARACTERIZATION
2.2.1 FTIR ANALYSIS

The Fourier transform infrared spectroscopy (FT-IR) study was carried out using Perkin Elmer FTIR – 1600 series infrared spectrometer. FTIR spectra was recorded in the range of 400-4000 cm⁻¹ with KBr pellet technique.

2.2.2 SURFACE PROPERTIES

The specific surface area was determined by nitrogen gas adsorption at 77 K using Surface Area Anlyzer (Nova 2200, Quantachrome- USA). The measurements were made after degassing under vacuum for 6 h. The specific surface area (SBET) was calculated by BET method [15].

2.2.3 SCANNING ELECTRO MICROSCOPY (SEM)

The surface morphology of chitosan was observed under a scanning electron microscope (JSM T20 JOEL, JAPAN). The sample was gold coated prior to SEM observation

2.3 KINETIC STUDY

Experimental set up is shown in Fig. 1. The apparatus consisted mainly of vertical cylindrical jacketed glass column (30 cm height and 4.5 cm inside diameter). The column was fitted with a G1 sintered-glass distributor with average diameter pores 5-10 microns. Next to gas distributor, a ball valve and rotametr were fixed to control air flow rate. Temperature was adjusted by passing hot water, thermostatically controlled, in the jacket around the column. Before each run, the column was filled with 0.4 dm^3 of fresh chromium solution at a certain concentration, followed by addition of a known mass of chitosan (M ,g) , adjusting the air flow rate(F, cm^3/ min) at temperature (T,^{0}C). The air flow rate was measured with a calibrated rotameter.

1- Glass cylindrical column
2- Sintered glass for air distribution
3- Glass jacket
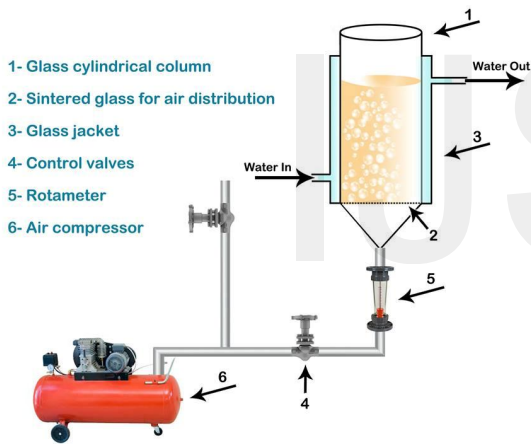4- Control valves
5- Rotameter
6- Air compressor

Fig 1. Gas stirring system.

The effects of the adsorbent mass (0.035-0.235 g), initial chrome concentration (30- 130 mg/dm^3) and air flow rates (240-800 cm^3/min) were investigated. The samples were taken at time intervals, centrifuged and the amount of the chromium adsorbed was calculated from the initial and final concentrations of chromium in the liquid phases. The chromium uptake by chitosan was calculated by the following equation.

$$q_t = \frac{(C_o - C_t)v}{M} \qquad (1)$$

Where q_t (mg/g) is the amount of adsorbed chromium at time t; v the volume of the solution (dm^3) , C_o and C_t are the initial and the final chromium concentrations at time t respectively (mg/dm^3) and M is the mass of adsorbent(g).

2.3.1 KINETIC MODELING

In order to investigate the adsorption kinetic of the adsorption of chromium on chitosan and optimized the design of a sorption system, it is important to establish the most appropriate correlation for the kinetic curves. There are many theories relating to adsorption kinetic and among the used models are Pseudo-First order, Pseudo – Second order, Elovich and Modified Freundlich models

2.3.1.1 PSEUDO FIRST ORDER EQUATION(LAGERGREN MODEL)

Lagergren [16] suggested a rate equation for the sorption of solutes from liquid solution. The pseudo first-order equation in generally expressed as follow:

$$\frac{dq_t}{dt} = k_1(q_e - q_t) \quad (2)$$

Integrating Eq. (2) and applying the boundary conditions $q_t = 0$ at t=0 and $q_t = q_t$ at t=t, gives:

$$\ln(q_e - q_t) = \ln q_e - k_1 t \quad (3)$$

Where q_e and q_t are the amount of chromium adsorbed at equilibrium and at time t (mg/g) respectively, and k_1 is the rate constant of the pseudo first- order adsorption (1/min).

2.3.1.2 PSEUDO SECOND ORDER EQUATION(HO MODEL)

If the rate adsorption is a second-order mechanism, the Pseudo second order equation kinetic rate equation is expressed as [17]:

$$\frac{dq_t}{dt} = k_2(q_e - q_t)^2 \qquad (4)$$

Where k_2 is the rate constant of sorption (g/mg.min)

Separating the variable in Eq. (4) and integrating by applying the boundary conditions

$$\frac{1}{q_e - q_t} = \frac{1}{q_e} + k_2 t \qquad (5)$$

Eq.(5) can be rearranged to obtain a linear form:

$$\frac{t}{q_t} = \frac{1}{k_2 q_e^2} + \frac{t}{q_e} \quad (6)$$

The initial sorption rate, h(mg/g min), at t =0 is defined as

$$h = k_2 q_e^2 \quad (7)$$

2.3.1.3 THE ELOVICH EQUATION

Elovich model [18] is a rate equation based on the adsorption capacity as:

$$\frac{dq_t}{dt} = \alpha e^{-\beta q_t} \quad (8)$$

The integration of the rate equation with the same boundary conditions as the Pseudo-first order, the Pseudo – second order equations become

$$q_t = \frac{1}{\beta}\ln(\alpha\beta) + \frac{1}{\beta}lnt \quad (9)$$

Where α is the initial adsorption rate (mg/g.min) and the parameter β is related to the extent of surface coverage and activation energy

2.3.1.4 MODIFIED FREUNDLICH MODEL

The modified Freundlich model a originally developed by Kuo and Lotse[19]

$$q_t = k_f C_0 t^{1/m} \quad (10)$$

Where kf the apparent adsorption rate constant (dm³/g.min), m is the Kuo-Lotse constant. The linear form of the modified Freundlich equation is given as

$$\ln q_t = ln(k_f C_0) + \frac{1}{m}lnt \quad (11)$$

2.3.2 ERROR ANALYSIS FOR KINETIC MODELS

The traditional approach of determining the kinetic parameters by linear regression of kinetic equations appears to give very good fits to the experimental data as most of their respective regression correlation coefficients (R^2) are close to unity. The use of R^2 is limited to solve linear forms of kinetic equation, which measures the difference between experimental and theoretical data in linearized plots only, but not the errors in non-linear form of kinetic curves. So, the applicability of the kinetic model to describe the adsorption process was further validated using error functions [20]. The error functions studied were as follows.

1- The sum of the absolute errors (SAE)
The sum of the absolute of the errors method can be represented by the following equation:

$$\sum_{i=1}^{N}\left|q_{t,cal} - q_{t,exp}\right|_i \quad (12)$$

2- The sum of the square of the errors (SSE)

The sum of the squares of the errors method can be represented by the following equation:

$$\sum_{i=1}^{N}\left(q_{t,cal} - q_{t,exp}\right)^2 \quad (13)$$

Where N is the number of points on a fitted experimental curve.

3. RESULTS AND DISCUSSION

3.1 Characterization of chitosan

The physical properties of chitosan (total surface area, average pore diameter, bulk density and porosity used in this study are shown in Table 1.

Table 1: Physical characteristics of chitosan

BET surface area m²/g	211.2
Average pore diameter µm	0.961
Bulk density g/ cm³	0.283
Apparent density g/ cm³	1.825
Porosity	0.845

3.1.1 SCANNING ELECTRON MICROSSCOPY

The SEM micrographs for chitosan are shown in Fig 2 at different magnifications (100, 250 and 700). It can be seen from Fig.2 that the chitosan display a rough surface and has irregular diameter in the range of 14.6 – 37.6 µm.
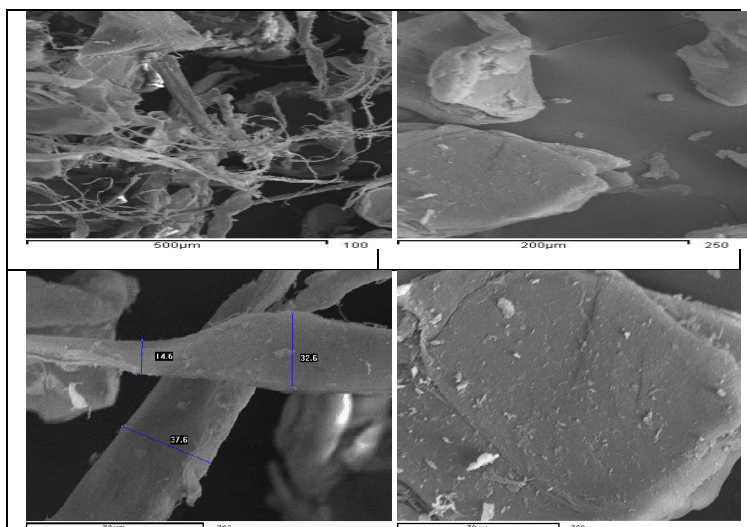
Fig 2 SEM for chitosan

3.1.2 FTIR ANALYSIS

The chitosan was characterized by FTIR spectroscopy for their chemical constitution. The IR spectra for the chitosan are shown in Fig. 3.
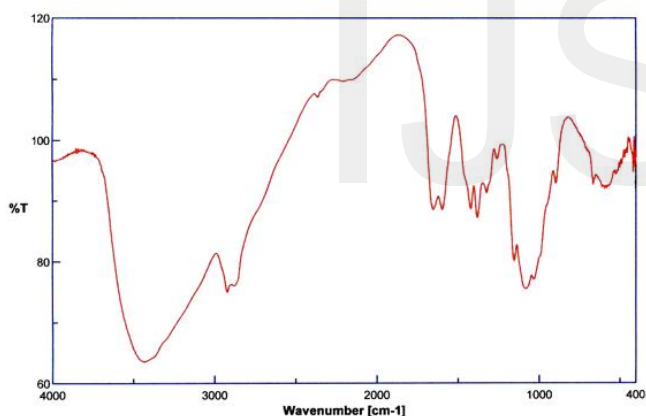

Fig 3. FTIR plot for chitosan

Band in the region of 3400- 3500 cm^{-1}, which must have been masked by the absorption, this band due to the OH group. The NH$_2$ stretching (amide II) peak at 1567 cm^{-1} representing the glucosamine functional group, appeared in the spectrum of chitosan powder. Another significant change is observed in the region from 1000 cm^{-1} to 1200 cm^{-1}, in this region chitosan presents a broad band centred at 1076 cm^{-1} associated with the stretching of C-O.In the region of 3000 cm^{-1} to 3700 cm^{-1} of the spectrum, chitosan exhibits a band corresponding to the stretching of OH groups. This band is broad because of the hydrogen bonds. The OH band overlaps the stretching band of NH as shown in Fig. 3.

3.2 EFFECT OF CHROMIUM INITIAL CONCENTRATION

The effect of initial chromium concentrations on the extent of adsorption on chitosan as a function of time is shown in Fig. 4. The amount of chromium adsorption increases with increasing initial chromium concentration. For instance the amount of chromium adsorbed at equilibrium increased from 99.354 to 239.99 mg/ g when chromium concentration increased from 30 to 130 mg/ dm^3. This may be attributed to an increasing concentration gradient acting as an increasing driving force to overcome all mass transfer resistances of the chromium molecules between the aqueous and solid phase, leading to an increasing equilibrium sorption until saturation is achieved.
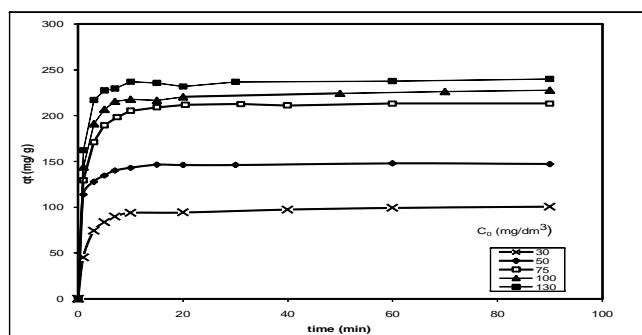

Fig.4 Effect of chromium initial concentration on the adsorption onto chitosan.(M=0.118 g ,T=30+2°C ,F 240 cm^3/min and pH 2.5)

3.3 EFFECT OF ADSORBENT DOSAGE

The amount of adsorbent used in adsorption is particularly important because it determines the sorbent–sorbate equilibrium in the system and can also be used to predict the treatment cost of the adsorption process. The effect of adsorbent dosage on the chromium removal was studied and the results presented in Fig. 5. The chromium removal decreased with an increase in adsorbent dosage. For instance, the quantity of chromium uptake at equilibrium decreased from 265.348 to 149.855 mg/g when the adsorbent weight increased from 0.035to 0.235 g.

It was found that the mass transfer decreases by increasing mass of adsorbent. This effect is probably due to the fact that for small masses, small amount of external mass surface is available for the adsorption of the chromium. Hence, on one hand, there is a large driving force from the chromium per unit surface area of chitosan. On other hand, the decrease of uptake with increase in the adsorbent mass can be attributed to the effect of the concentration of solid upon magnitude on the driving force per unit area in the liquid phase. At greater solute gradients with smaller solid concentration and hence lower external surface area due to large contacts between the crowding solid particles which leads to decrease the amount of adsorbed Cr. The decrease of Cr uptake with the mass of

chitosan can also, be understood mathematically through the relation: $q_t = (C_0-C_t) \, v \, /M$ (Eq. 1) by increase M at constant (C_0 - C_t), q_t will decreased [21].
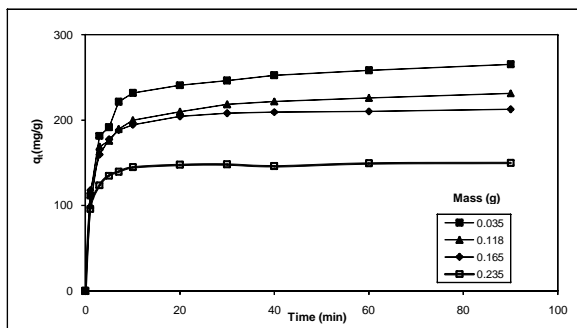

Fig5 Effect of chitosan mass on the adsorption of chromium (C_o=100mg/dm^3,T=30+2°C ,F 240 cm^3/min and pH 2.5)

3.4 EFFECT OF AIR FLOW RATE

Figure 6 shows the plot of qt versus t for the adsorption of chromium onto chitosan using various air flow rates. As shown in Fig. 6, the removal of chromium is decreasing as the air flow rates increases. The amount of chromium adsorbed reach to 311 mg/g at 216 cm^3/min, while at 800 cm^3/min only 208 mg/g of chromium was removed from the solution.

It can be concluded that the effects of air flow rate on the uptake of chromium are not significant for chromium removal. As the air flow rate increases, the suspension may not become homogeneous due to the rapid agitation which can leads to decrease the adsorption due to decrease the contact between chromium and chitosan particles.. Similar results have been previously reported[22].
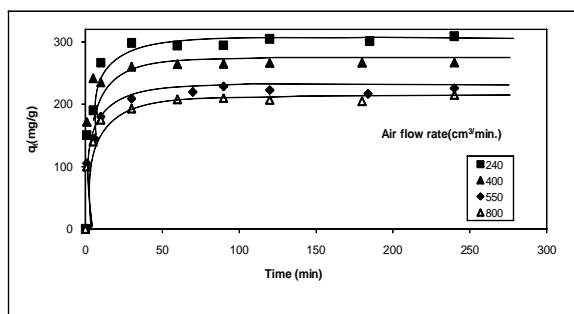

Fig. 6 Effect of air flow rate on the adsorption of chromium onto chitosan (M=0.035 g, T=20+2°C, Co=100mg/dm^3 and pH 2.5)

3.5 Adsorption kinetics models

Several kinetic models including pseudo-first order of Lagergren, models were tested for simulation of the experimental data. pseudo-second-order, Elovich, pore diffusion and modified Freundlich The linear plots $\ln(q_t–q_e)$ vs. t, t/q_t vs. t, q_t vs. ln t and ln q_t vs. ln t,. allowed checking the validity of the different models (Pseudo First order, Pseudo Second order, Elovich and Modified Freundlich models respectively) . The kinetic parameters calculated from Eqs. 3,6,9 and 11 for the adsorption of chromium at different initial chromium concentrations, adsorbent mass and air flow rates are given in Tables 2. From Tables 20 the pseudo-second-order seems to be the most appropriate, owing to the highest correlation coefficients recorded (always above 0.99) The other three models failed to described the experimental data well, as indicated by consistently lower $R^2 < 0.9$, implying that the adsorption kinetics of the chromium followed a pseudo-second-order model.

Table 2. Kinetic parameters of Pseudo-first order model Fitting chromium adsorption onto chitosan.

Variables		K_L (1/min)	$q_{e,L}$ (mg/g)	$q_{e, exp.}$ (mg/g)	R^2
Mass (g)	0.035	0.0518	102.09	265.35	0.82
	0.118	0.055	87.217	231.57	0.85
	0.165	0.0748	61.873	212.85	0.85
	0.235	0.0742	29.41	149.86	0.74
Initial Concentration (mg/dm^3)	30	0.0649	51.487	99.33	0.93
	50	0.058	76.577	154.4	0.91
	75	0.0514	102.165	203.31	0.91
	100	0.55	87.217	231.57	0.85
	130	0.0896	82.319	239.86	0.86
Air flow rate (Cm^3/min)	240	0.0451	81.789	311	0.72
	400	0.0599	34.316.	267.5	0.73
	550	0.0362	69.215	226	0.67
	800	0.0527	67.05	216	0.81

Table 3 .Kinetic parameters of Pseudo-second order model Fitting chromium adsorption onto chitosan.

Variables		K_2 g/mg.min	q2 mg/g	$q_{e,exp.}$ mg/g	R^2
Mass (g)	0.035	0.0024	270.27	265.35	0.99
	0.118	0.0029	232.56	231.57	0.99
	0.165	0.0057	212.77	212.85	0.99
	0.235	0.014	149.25	149.86	0.99
Initial Concentration (mg/dm³)	30	0.0047	101.01	99.33	0.99
	50	0.0031	156.25	154.4	0.99
	75	0.0021	204.08	203.31	0.99
	100	0.0029	232.56	231.57	0.99
	130	0.0032	238.09	239.86	0.99
Air flow rate (Cm³/min)	240	0.0033	312.5	311	0.99
	400	0.0114	270.27	267.5	1
	550	0.0049	227.27	226	0.99
	800	0.0045	212.77	216	0.99

Table 4 . Kinetic parameters of Elovich model Fitting chromium adsorption onto chitosan.

Variables		A (mg/g.min)	β (-)	R^2
Mass (g)	0.035	2,826	0.0321	0.90
	0.118	3,555	0.0385	0.89
	0.165	21,757	0.0508	0.87
	0.235	48,747	0.0965	0.78
Initial Concentration (mg/dm³)	30	225	0.0672	0.92
	50	510	0.047	0.96
	75	744	0.0369	0.96
	100	3,555	0.0385	0.89
	130	14,535	0.04419	0.90
Air flow rate (Cm³/min)	240	5,094	0.0339	0.8
	400	34,596	0.0681	0.83
	550	2,009	0.0416	0.86
	800	258	0.0316	0.85

Table 5 . Kinetic parameters of Modified Freundlich model Fitting chromium adsorption onto chitosan.

Variables		m (-)	k_f (dm³/g.min)	R^2
Mass (g)	0.035	6.06	1.4048	0.82
	0.118	6.43	1.273	0.81
	0.165	8.57	1.377	0.82
	0.235	12.08	1.108	0.74
Initial Concentration (mg/dm³)	30	4.134	1.33	0.81
	50	5	1.408	0.91
	75	5.152	1.245	0.91
	100	6.43	1.273	0.81
	130	8.103	1.128	0.84
Air flow rate (Cm³/min)	240	6.622	1.502	0.77
	400	14.34	1.824	0.83
	550	6.006	1.061	0.83
	800	3.469	0.645	0.79

From results of calculated correlation coefficients (Tables 6-8) , it seems that the Pseudo Second order model is the most suitable model to satisfactorily describe the studied sorption system. Indeed the highest R^2 values and the lowest SSE and SAE values were found when modelling the kinetic data.

Table 6 Values of error analyses of kinetic models for adsorption of chromium onto chitosan at different chitosan mass

Mass of Chitosan	Pseudo First order	Pseudo Second order	Elovich	Modified Freundlich
M =0.035 g				
SSE	2.8×10^5	554.25	2049.82	3880.91
SAE	1652.3	60.76	111.64	168.5
M =0.118 g				
SSE	2.2×10^5	283.85	1465.95	2679.31
SAE	1462	45.01	98.63	144.16
M =0.165 g				
SSE	2.3×10^5	89.94	1068.04	1622.98
SAE	1504	21.99	85.138	110.62
M =0.235 g				
SSE	1.45×10^5	63.7	565.24	705.79
SAE	1200.8	20.35	63.5	74.09

Table 7 Values of error analyses of kinetic models for adsorption of chromium onto chitosan at different initial concentration of chromium

Concentration	Pseudo First order	Pseudo Second order	Elovich	Modified Freundlich
C_o= 30mg/ dm³				
SSE	4.4x10⁴	52.6	390.68	1096.24
SAE	619.55	15.99	51.65	91.99
C_o= 50mg/ dm³				
SSE	1.34x10⁵	65.46	5311.09	933.99
SAE	1155.7	18.21	163.16	78.77
ARE				
C_o= 75mg/ dm³				
SSE	3.21x10⁵	487.33	507.91	1415.67
SAE	1874	51.93	58.5	97.71
C_o= 100mg/ dm³				
SSE	3.25x10⁵	70.87	1465.95	2679.3
SAE	1797	22.05	98.626	144.16
C_o= 130 mg/dm³				
SSE	3.9x10⁵	359.6	1011.26	1615
SAE	1969.9	2529.9	82.24	111.76

Table 8 Values of error analyses of kinetic models for adsorption of chromium onto chitosan at different air flow rates

Flow rate	Pseudo First order	Pseudo Second order	Elovich	Modified Freundlich
F=240(cm/min)				
SSE	4.62x 10⁵	2529.9	3886.28	5575.87
SAE	2014.5	91.86	157.56	186.83
F=400(cm/min)				
SSE	4.84x 10⁵	395.29	809.94	870.96
SAE	2083	36.59	73.39	74.55
F=550(cm/min)				
SSE	2.39x10⁵	1459.9	1723.938	2882.879
SAE	1449.8	78.38	112.8416	137.96
F=800(cm/min)				
SSE	1.94x10⁵	430.29	3065.47	7523.87
SAE	1310.12	42.66	152.9	222.399

The models prediction for the change in chromium concentration with the time are compared with the experimental data in Figs 7,8. Its observed that the Pseudo second-order equation provides the best correlation for all of the sorption process. The pseudo first-order equation does not fit to the experimental data for the adsorption of chromium.
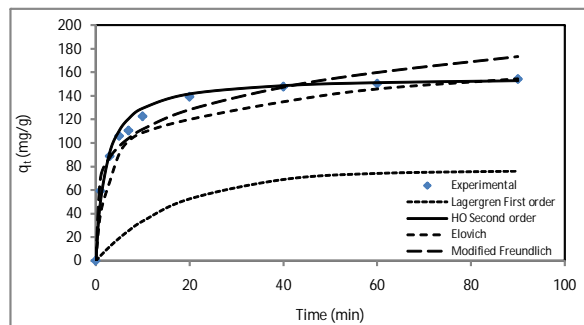

Fig. 7. Comparison experimental and calculated kinetic profile using several kinetic models. (C_o=50mg/dm³ ,M=0.118 g ,T=30±2°C ,F 240 cm³/min and pH 2.5)

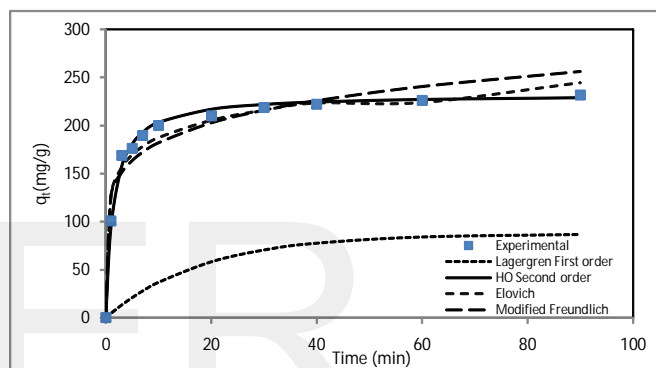Fig 8. Comparison the experimental and the calculated kinetic profile using several kinetic models. (C_o=100mg/dm³, M= 0.118 g, T=30±2°C ,F 240 cm³/min and pH 2.5)

This suggest that the adsorption systems studied belong to the second-order kinetic model, based on the assumption that the rate limiting step may be chemical sorption or chemisorptions involving valency forces through sharing or exchange of electrons between adsorbent and adsorbate.

4 Conclusions

Batch experiments were conducted to determine the adsorption ability of hexavalent chromium onto chitosan using air stirring techniques. This work confirms that, chitosan was found to be an effective adsorbent for the removal of Cr (IV) from aqueous solutions. The study showed that time, concentration of chromium, chitosan mass and air flow rate influence the adsorption process. The kinetic data indicated

that the sorption kinetic of chromium onto chitosan using air stirring follows the pseudo-second-order model.

References

[1] Sarin, V., Pant, K.K., Removal of chromium from industrial waste by using eucalyptus bark. Bioresour. Technol. 97, 15–20, 2006.

[2] Mohan, D., Singh, K.P., Singh, V.K., Removal of hexavalent chromium from aqueous solution using low-cost activated carbons derived from agricultural waste materials and activated carbon fabric cloth. Ind. Eng. Chem. Res. 44, 1027–1042, 2005.

[3] Levankumar, L., Muthukumaran, V., Gobinath, M.B., Batch adsorption and kinetics of chromium (VI) removal from aqueous solutions by Ocimum americanum L. Seed pods. J. Hazard. Mater. 161, 709–713, 2009.

[4] D. Mohan, C.U. Pittman Jr., Activated carbons and low cost adsorbents for remediation of tri- and hexavalent chromium from water, J. Hazard. Mater. B137 , 762–811, 2006.

[5] J. Li, Q.-y. Yue, et al., Adsorption of chromium (vi) from aqueous solution on bentonite modified by cationic polymers, Huanjing Kexue 30 ,1738–1743, 2009.

[6] A. Atia, Adsorption of chromate and molybdate by cetylpyridinium bentonite, Appl. Clay Sci. 41 ,73–84, 2008.

[7] Guang L., Xiaogang Y. and Gance D., " Simulation of effects of the configuration of gas distribution on gas gas-liquid flow and mixing in a bubble column " Chem. Eng. Sci. 64,5104-5116, 2009.

[8] Nassar M.M. Energy consumption and mass transfer during adsorption using gas and mechanical stirring system Wat. Res. 32: 3071-3079, 1998.

[9] Decker W.D. Bubble column reactors. Wiley, New York, USA, 1992.

[10] Nassar, M M, Farrag T E and Joseph Y Farah, " Gas sparged adsorbed for decolourization dye effluent" Eurasian Chem Tech Journal ,9,1:31-36, 2007.

[11] Jia Y., Wang R. and Fane A. G. ,Atrazine adsorption from aqueous solution using powder activated carbon – Improved mass transfer by air bubbling agitation, Chem Eng Journal 116,53-59, 2006.

[12] M M.Nassar, M.S.El-Guendy and A A. Wahabi "Enhancing adsorption of dyes onto clay in Bubble Asorber" Adsorption Science & Technology, 30,. 7, 567-577, 2014.

[13] Snell, F.D. , Snell, C. T., Colorimetric Methods of Analysis , third ed., vol. 2, D. Van Nostrand Company , New York, Toronto, 1959.

[14] Arnold,E.Greenberg ; Lenore, S. Clesceri ; and Andrew, D. Eaton, Standard Methods For The Examination Of Water And Wastewater, 18th Edition, 1992.

[15] S. Brunauer, P.H. Emmett, E. Teller, Adsorption of gases in multi molecular layers, J. Am. Chem. Soc. 60 ,309–319, 1938.

[16] Lagergren, S. ,About the theory of so-called adsorption of soluble substances. Kungliga Svenska Vetenskapsakademiens Handlingar, Band. 24 (4): 1–39, 1898.

[17] Y.S. Ho, G. McKay, Pseudo-second order model for sorption processes,Process Biochem. 34 , 451–465, 1999.

[18] Cheung, C.W., Porter, J.F., McKay, G., Elovich equation and modified second–order equation for sorption of cadmium ions onto bone char, J. Chem. Technol. Biotechnol. 75, 963–970, 2000.

[19] Kuo, S. and Lotse, E.G. " Kinetics of phosphate adsorption and desorption by hematite and gibbsite", Soil Sci. Soc. Am. J. 116: 400–406 , 1973.

[20] Wang,Z., Yue,T., Yuan, Y., Cai,R., Niu,C. and Guo C." Kinetics of adsorption of bovine serum albumin on magnetic carboxymethyl chitosan nanoparticles" International Journal of Biological Macromolecules 58 ,57– 65, 2013.

[21] Choy, K.K.H.; Ko, D.C.K; Cheung, C.W.; Porter J.F. and McKay G. ,Film and intraparticle mass transfer during the adsorption of metal ions onto bone char. J. Colloid Interface Sci. 271:284–295, 2004.

[22] Kabbashi,N.A., Atieh, M.A., Al-Mamun1,A., Mirghami1, M. E. S.,Alam, M, Z. and Yahya,N. "Kinetic adsorption of application of carbon nanotubes for Pb(II) removal from aqueous solution" Journal of Environmental Sciences 21, 539–544, 2009.